

INFLUENCE OF PROCESS VARIABLES ON THE MICROSTRUCTURE OF LOW PRESSURE PLASMA SPRAYED TUNGSTEN

Rajan Bamola*, Ray Hendrichsen, Albert Sickinger*****

***Surface Modification Systems Inc. Santa Fe Springs, CA 90670**

****GE Medical Systems, Warrensville Heights, OH 44128**

***** ASA Consulting, Irvine, CA, 92604**

ABSTRACT

Low Pressure Plasma Spraying (LPPS) is a well established method of applying dense, adherent refractory alloys as protective coatings. However, little work has been done using LPPS to form coatings and free standing forms of tungsten with microstructures and densities approaching that of traditional powder consolidation techniques such as sinter forging. This paper presents results from a systematic study of the influence of LPPS process variables on the density and microstructure of tungsten deposits. Plasma gas combinations, particulate size, spray distance and chamber pressures were investigated and related to the microstructure and density of deposits. It was found that refined equiaxed grains, smaller than those found in sinter-forging, were present. Densities of over 94% could be consistently achieved using tightly controlled parameters.

INTRODUCTION

Low Pressure Plasma Spray (LPPS) is a well established technique of applying refractory coatings; primarily of nickel based superalloys. The reader is referred to several sources describing this technique^{1,2,3,4}. Briefly; the equipment is constructed from a water cooled torch consisting of a tungsten cathode and annular copper anode. Plasma is created by passing gases between the anode and cathode, the annulus allows the plasma to exit the torch with considerable velocity and enthalpy. Finely divided powder can then be strategically injected into the plasma leading to various thermal and velocity histories for the particles. The process is generally conducted in air. A variation is when the torch is enclosed in a water cooled chamber and the effected at reduced pressures (LPPS). In the case of LPPS a transferred arc between the workpiece and torch can be introduced prior to and during spraying, cleaning the substrate and introducing additional heating of the workpiece. Amongst the benefits touted for this process over conventional air plasma spraying are; improved densities, improved bond strengths, low gas content in metallic coatings, high deposition rates and the ability to form free-standing near net shapes. These features lead to the possible use of this process to create coatings and free forms of refractory and reactive materials such as Tungsten, Molybdenum, and Rhenium. McKechnie has written several papers on LPPS of Tungsten claiming densities from 93 to 97% however, little detail of the processing technology is

given⁵. In order for LPPS to be established as a process for consolidation of refractories such as tungsten, deposit densities comparable to those obtained from traditional powder consolidation techniques such as sinter-forging will have to be obtained. Sinter forging of tungsten will generally lead to densities of 94-95%. LPPS offers several advantages over traditional methods such as microstructural and properties uniformity over a range of sizes and shapes, smaller equipment footprint and less processing steps.

Potential applications of Tungsten and its alloys are in ballistics, space hardware, radiation shielding, counterweights, electronic packaging, medical imaging, and Tokamak reactor shields.

One of the objectives of this study was to demonstrate the ability to obtain a fully recrystallized equiaxed grain structure as opposed to the conventional splat like morphology typically observed during LPPS processing. Splat-like structures contain considerable intersplat porosity (Figure 1) restricting use in high end applications.

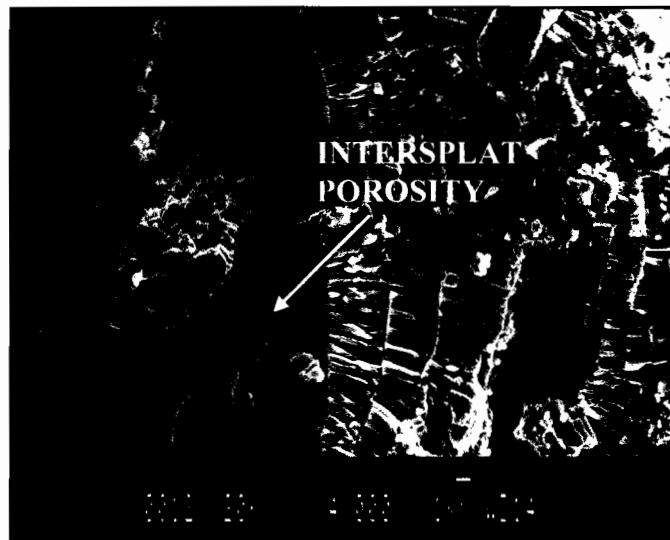


Figure 1: Conventional LPPS Tungsten cross-sectional Fractograph

Densification techniques for LPPS coatings and free forms are vacuum heat treatment and hot isostatic pressing. However, such techniques invariably lead to grain growth and subsequent pore entrapment limiting final densities that can be achieved. The better strategy would be to use the inherent processing strengths of LPPS to achieve the required grain structure and densities in one step processing. This study explores strategies utilizing process variable manipulation in order to create equiaxed high density deposits of Tungsten.

EXPERIMENTAL

An Electroplasma built LPPS system equipped with an O3CA torch was used in this study. Four axis of motion were available. Typical deposition sequence were: 1) Pump down to between 20 – 26 Pa (150-200 millitorr), 2) backfill to the appropriate chamber pressure, 3) sputter clean substrate using reverse arc, 4) Spray deposit coating 5) cool to 100°C maximum and remove the coated piece. Substrates were 100 mm diameter by 15 mm thick (4"OD by 5/8" thick) TZM (Molybdenum alloy) discs. During spraying the substrate temperature was over 1100°C

Process variables investigated were: 1) the effect of powder size and distribution, 2) spray distance, 3) chamber pressure and 4) plasma power. Initial development work optimized hardware and a basic spray recipe was then improved on by optimizing each process variable.

Coating cross-sections were prepared by standard metallographic procedures. An electrolytic etch of sodium hydroxide was used to reveal the grain structure of the coating. Both optical and scanning electron microscopy was used. Densities were measured by Archimedes principle on tungsten samples prepared by acid dissolution of the substrate.

RESULTS

EFFECT OF POWDER SIZE AND DISTRIBUTION

Figure 2 shows the powder distribution curves and the corresponding microstructures. Table 1 presents the Archimedes density data for the four conditions.

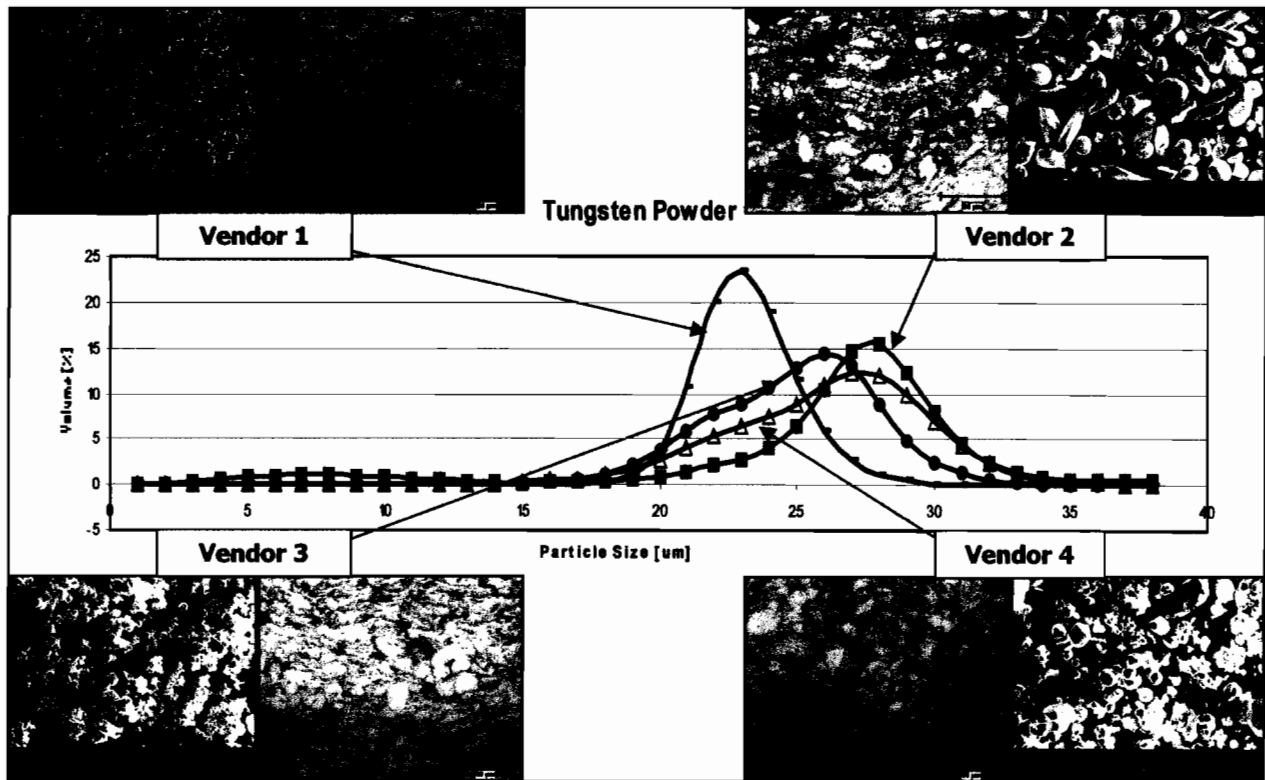


Figure 2: Powder Distribution, Morphology and Corresponding Cross-Section

Table 1: Effect of Particle Size and Distribution on Density

	Vendor 1	Vendor 2	Vendor 3	Vendor 4
Density [%]	90.6	84	88	87

Powders obtained from vendors 2, 3 and 4 were all classified as $-45\mu\text{m} +5\mu\text{m}$. Vendor 1 supplied powder ranging from $5-26\mu\text{m}$. Two observations were relevant; 1) The finer powder and tighter size distribution from vendor 1 resulted in a denser coating structure, and 2) the $-45\mu\text{m} +5\mu\text{m}$ powders all had differing powder morphologies and frequency plots. This variation in powder size and morphology results to an obvious difference in microstructure and density. The densities can be roughly related to the D_{50} of the frequency plots. In the case of vendor 2 the presence of larger particles results in a lower melting and packing efficiency reducing the density of the coating.

EFFECT OF SPRAY DISTANCE

The powder obtained from vendor 1 was used to spray coatings at 8 kPa (60 Torr) at 150 mm, 250 mm, and 300 mm distance between the substrate and gun. Figure 3 presents cross-sectional optical metallographs of the coatings. Table 2 presents densities obtained at the various spray distances.

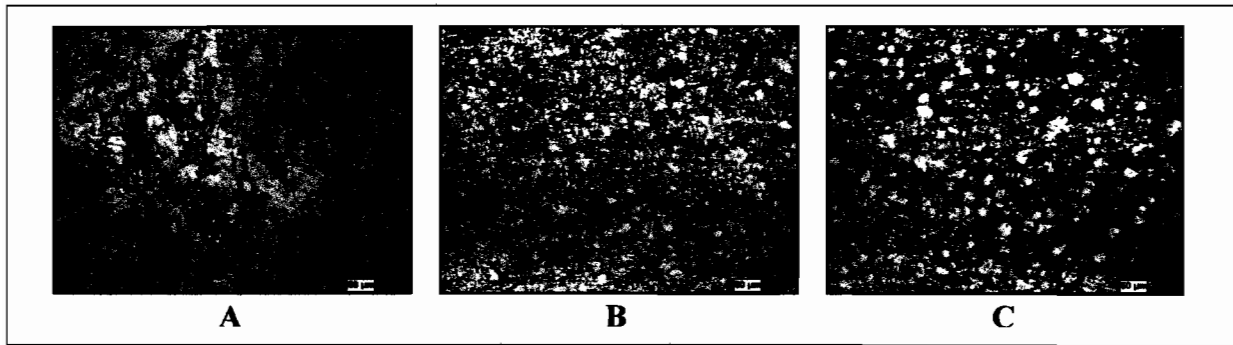


Figure 3: Microstructure of Coatings at A = 150 mm, B = 250 mm, C = 300 mm

Table 2: Effect of Spray Distance on Density

Distance in [mm]	150	250	300
Density [%]	92.7	90.7	87

Improvements in microstructure and density are realized with a decrease in spray distance to 150 mm. At 300 mm many spherical particles were observed in the structure. These result from resolidification of the smaller particles during flight. At 250 mm the number of resolidified particles decreases with a subsequent increase in density. At 150 mm a recrystallized microstructure results with densities approaching 93%. Recrystallization of the splat structure is thought to occur as a result of the contribution of thermal energy from the plasma as the gun is brought closer to the substrate. The recrystallized coatings structure consisted of elongated grains aligned in the direction of heat extraction.

EFFECT OF CHAMBER PRESSURE

Coatings were applied at 4, 8, and 26 kPa (30, 60, and 200 Torr) chamber pressure while maintaining constant power and powder feed rate. Since the plasma stream constricts at higher pressures, the spray distance had to be adjusted to obtain the best coating at a particular pressure. Figure 4 and Table 3 presents the microstructure and density data for the three conditions.

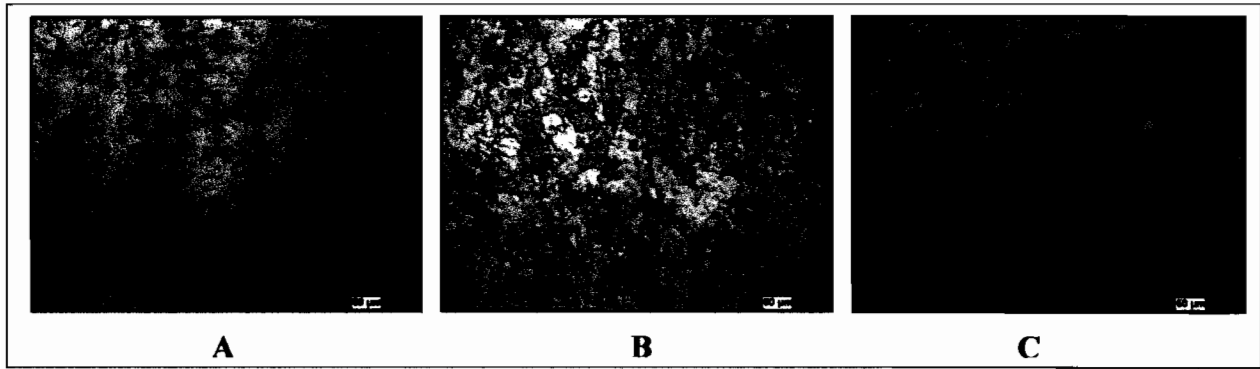


Figure 4: Effect of Pressure on Microstructure at A = 4 kPa, B = 8 kPa, and C = 26 kPa

Table 3: Effect of Chamber Pressure on Density

Chamber Pressure [kPa]	4	8	26
Density [%]	93.4	92.7	89.4

At both 4 and 8 kPa (30 and 60 Torr), recrystallization of the coating occurs, while a fine splat-like structure is present at 26 kPa (200 Torr). It is interesting to note that although the sample at 26 kPa was applied at the same power level and at an even closer spray distance, the splat structure is still retained. This observation indicates that both high particle velocities and high substrate temperatures are requirements in LPPS to eliminate the splat-like structures and achieve recrystallization. Lower chamber pressures exert less braking forces on the particles therefore higher particle velocities are achieved in these cases, leading to better packing densities and greater ease of surface and grain boundary diffusion.

EFFECT OF POWER LEVEL

Results from the previous parameter studies indicate densities increase with 1) fine particles with tight distribution, 2) high substrate temperatures, and 3) high particle velocities. This section of the investigation exploited the results from the preceding studies by applying coatings with an even finer particle size (D_{50} below 15 μm) at chamber pressures of 30 Torr and using power levels of 88 kW, 93 kW and 100 kW. Figure 5 and Table 4 present the microstructure and density data at these conditions.

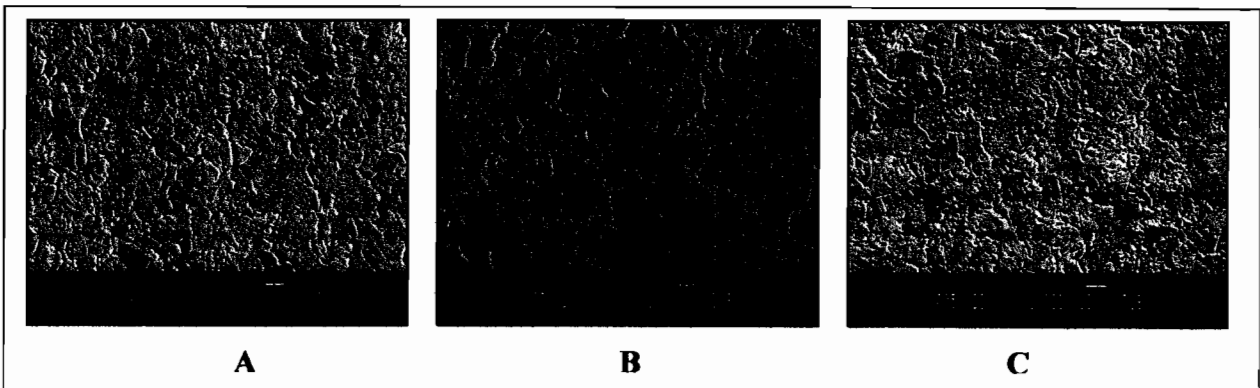


Figure 5: Effect of Power on Microstructure at A = 88 kW, B = 93 kW, and C = 100 kW

Table 4: Effect of Power on Density

Power [kW]	88	93	100
Density [%]	94.5	94.5	94.4

All cross-sections show a fine equiaxed grain structure with densities comparable to those found in powder sinter-forging. The primary difference between the 3 conditions is the slight increase in grain size and entrapped porosity with an increase in power level. The 88 kW specimen showed fewer pores slightly larger in diameter than the 93 kW specimen which had more pores with smaller diameters. The slight decrease in density of the sample sprayed at 100 kW can be attributed to the higher distribution of larger pores in this specimen.

COMPARISON WITH SINTER FORGING

A sample of commercially available sinter-forged tungsten-5% rhenium on TZM was mounted and metallographically prepared together with a LPPS prepared sample with similar composition. The microstructures are presented in Figure 6. Two features are apparent. The LPPS sample has smaller grain size compared with sinter forged sample. Image analysis calculated average grain sizes of 8 μm and 18 μm for the LPPS and sinter forged specimen respectively. The sinter forged specimen also shows much bigger pores than the LPPS sample. The respective densities of the LPPS and the sinter forged specimen are 94.7% and 93.6%.

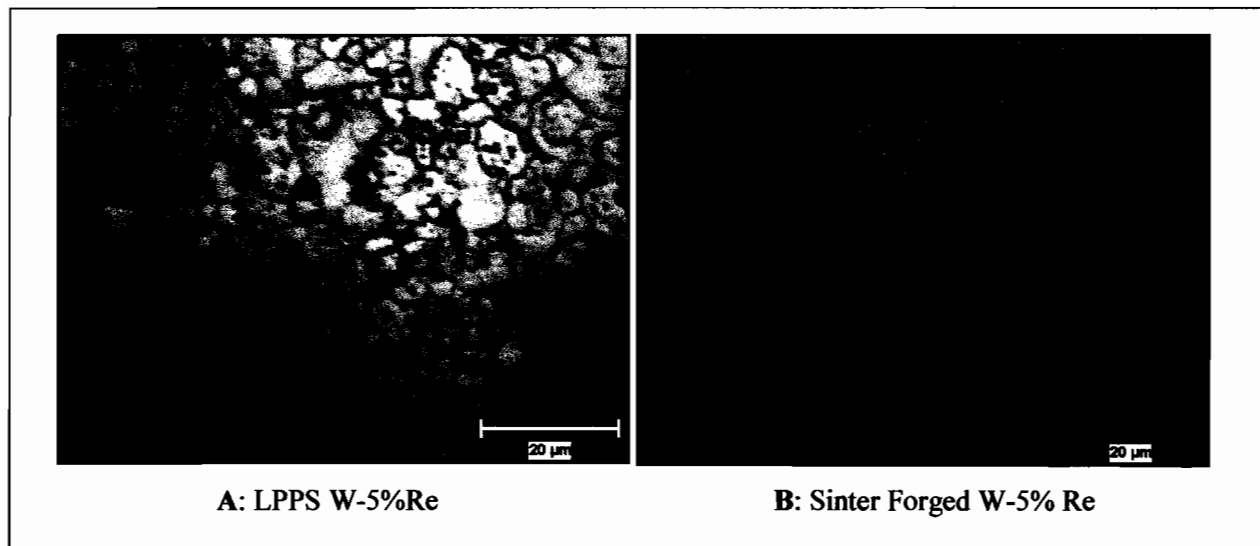


Figure 6: Comparison of A) LPPS and B) Sinter Forged Tungsten 5% Rhenium

DISCUSSION

An intensive study into the effects of process variables on the microstructure and density of tungsten coatings has been carried out. The predominant factor in achieving high density tungsten coatings is control of the powder size and distribution since other variables such as power level, chamber pressure

and spray distance can be easily manipulated. The large influence of the powder size is a result of the high density of tungsten; 19.3 g/cm^3 . To illustrate this point consider the following. A particle with an equivalent diameter of $10 \text{ }\mu\text{m}$ has a mass of $1.01 \times 10^{-8} \text{ g}$ whereas a particle with a diameter of $20 \text{ }\mu\text{m}$ has a mass of $8.08 \times 10^{-8} \text{ g}$. The heat required to melt a particle can be estimated from

$$\Delta H = mC_p\Delta T \quad (1)$$

The ratio of $\Delta H_{20\mu\text{m}}/\Delta H_{10\mu\text{m}}$ gives a value of 8. This means that approximately 8 times more heat is required to raise the temperature of a $20 \text{ }\mu\text{m}$ particle to the same level as a $10 \text{ }\mu\text{m}$ particle. This is non trivial when one considers the spread in conventional LPPS powder distributions is more than $30 \text{ }\mu\text{m}$. Furthermore, the powder size and therefore their mass have an effect on the terminal velocities that can be achieved. Smith has measured particle velocities in LPPS as a function of size and mass and concluded heavier particles have slower acceleration and deceleration than lighter particles⁶. Heavier particles also had lower peak velocities. The velocity and size of the particles also determine the packing density in the coatings. Assuming a disc like platelet on impact with diameter D , the coordination number is then 12, the porosity can be roughly approximated in the form of a triangular pie like structure with each side $1/8\pi D$ and splat height h , volume of this structure is the area of the equilateral triangle formed multiplied by the splat height

$$\text{Volume} = (1/2)(1/64)\pi^2 h D^2 \sin(60^\circ) \quad (2)$$

Again taking a 20 and $10 \text{ }\mu\text{m}$ particle and assuming the particle spreads to $4D$, h will then be $D/24$ (from conservation of mass). Substituting for D in equation 2 for the sizes in question leads to interstice porosity of $2.22 \times 10^{-11} \text{ cm}^3$ and $2.78 \times 10^{-12} \text{ cm}^3$ for the 20 and $10 \text{ }\mu\text{m}$ sized particles respectively. This demonstrates why the densities are higher of coatings formed from finer powders. Furthermore, it is much easier to bridge the smaller pores with molten liquid or flow from low viscosity superheated splats from subsequent passes contributing to further density enhancement. It is interesting to note that the porosity in Figure 5 is caused by pore entrapment in grains and along grain boundaries as in classical powder sintering rather than intersplat porosity as in Figure 1. It is also relevant that the recrystallized structures obtained by using coarser powder at 150 mm spray distance and 4 kPa (30 Torr) (Figure 4 A), does not have as high a density as those with equiaxed structures (Figure 5 A-C). It is obvious the recrystallization mechanism is different in these two cases. A possible explanation could be: in the case of Figure 4 the heat for grain formation is provided by the plasma torch hence the elongated grains, whereas in Figure 5 the spray distance was longer, therefore, the substrate received less heat, grain formation was more dependant on having a high packing density (high surface energy) where rapid diffusion could occur resulting in a more classical powder metallurgy sintering mechanism, however, on a condensed time scale. Another important consequence of using finer particles with a very tight distribution is that more uniform heating and increased melting will occur leading to increased densification by viscous flow. With larger particles there is a tendency to superheated surfaces on particles leading to localized neck formation between splats. More detailed analysis would be needed to verify this theory. These findings suggest that lowering the powder size further and increasing their velocity and decreasing the deposit temperature during spraying should limit the grain growth and thereby further increase density. However, equipment considerations such as the powder feeder and nozzle designs will eventually limit the size and velocity that can be achieved. In comparison to sinter-forging the faster heating and cooling cycles in LPPS have the beneficial effect of limiting grain growth and hence pore evolution.

CONCLUSIONS

The microstructure of tungsten deposits formed in LPPS is strongly influenced by processing variables. Under tight processing conditions, deposits of tungsten matching the microstructure and density of those found in powder sinter forging can be formed using LPPS. The predominant variable affecting density is powder size and distribution.

REFERENCES

- 1) E. Muelberger, Proceedings of the 7th International Metal Spraying Conference, London, United Kingdom, 1973, pp. 245-256
- 2) R. Dekumbis, P. Huber, M. Villat, Proceedings of the 10th International Thermal Spraying Conference, Essen, Germany, 1983, pp. 153-161
- 3) E. Lugscheider, 1st Plasma-Technik Symposium, Lucerne, Switzerland, 1988, pp.30-35
- 4) J.R. Rairden, M.R. Jackson, M.R. Henry, Proceedings of the 10th International Thermal Spraying Conference, Essen, Germany, 1983, pp. 205-208
- 5) T. McKechnie et al; Proceedings of the 5th National Thermal Spray Conference, Anaheim, CA, 1993, pp 297-301
- 6) M. Smith, 1st Plasma-Technik Symposium, Lucerne, Switzerland, 1988, pp 77-85